NUMERICAL TREATMENT OF MULTIPLE BIFURCATION POINTS

Reijo Kouhia* **and Martti Mikkola†**

*Laboratory of Structural Mechanics, Helsinki University of Technology
P.O. Box 2100, FIN-02015 HUT, Finland
e-mail: reijo.kouhia@hut.fi, web page: http://www.hut.fi/~kouhia/
†Laboratory of Theoretical and Applied Mechanics, Helsinki University of Technology
P.O. Box 1100, FIN-02015 HUT, Finland
e-mail: martti.mikkola@hut.fi, web page: http://www.hut.fi/Units/Dynamics/

Key Words: continuation algorithm, multiple bifurcation, branch switching, FEM

Abstract. *Branch switching procedures which are capable to handle critical points with coincident or nearly coincident buckling loads in a geometrically non-linear continuation process are presented. The proposed branch switching algorithm is based on a Liapunov-Schmidt-Koiter-type asymptotic reduction. Numerical examples of some plate and shell structures are shown.*

1 INTRODUCTION

Procedures to handle simple critical points on an equilibrium path of elastic structures are now well established.[1–7] Detection and location of a critical point can be done either during the incrementing process, or by a direct computation of an suitable augmented equilibrium equations.[8,9] These direct techniques have only been used to locate simple critical points. It is questionable if the overall efficiency of these algorithms is better than the standard incremental technique. In addition, the incremental technique can also provide more information to the analyst.

To branch out from the critical point onto the post-buckling range, an approximation to the path tangent is needed. For simple bifurcations there exists only one crossing path and the treatment is quite straightforward.

In the case of coincident critical points the situation is much more complex and only a few papers exist.[10–13] In this paper an approach which uses the Liapunov-Schmidt-Koiter type reduction technique is presented.

In recent years considerable progress has been made in the the application of group theoretic methods to the non-linear bifurcation analysis of symmetric structures.[14,15] The group representation theory helps in finding an optimal set of basis vectors which reflect the symmetry of a given problem. In formulating the numerical procedure with respect to the symmetry adapted basis offers several advantages: a dimensional reduction of the problem size due to the global decoupling of equilibrium equations and above all improves numerical conditioning of the equation system to be solved.

2 BASIC CONTINUATION ALGORITHM

Discretization of the quasi-static equilibrium equations expressing the balance between external and internal forces results in an equation of the form:

$$\boldsymbol{f}(\boldsymbol{q},\lambda) \equiv \boldsymbol{p} - \boldsymbol{r} = \boldsymbol{0}, \tag{1}$$

where $\boldsymbol{p}$ is the external load vector. If the finite element method is used in the discretization process, the internal force vector $\boldsymbol{r}$ follows from the assembly operation of the element contributions

$$\boldsymbol{r}^{(e)} = \int_{V^{(e)}} \boldsymbol{B}^T \boldsymbol{s} dV.$$

The vector $\boldsymbol{s}$ contains the stress components. The strain-displacement matrix $\boldsymbol{B}$ is defined by $\delta \boldsymbol{e} = \boldsymbol{B}\delta\boldsymbol{q}$, where the column vector $\boldsymbol{e}$ contains the strain components.

Usually the applied loading is assumed to depend linearly on a single parameter, i.e. the load parameter λ, such that $\boldsymbol{p} = \lambda \boldsymbol{p}_r$, where $\boldsymbol{p}_r$ is the reference load vector.

Solution of the equation system (1) forms a one-dimensional equilibrium curve in an $N+1$ dimensional displacement-load parameter space, where N is the dimension of the state space, i.e. the number of dof's in the particular finite element model. Procedures

to trace the one dimensional equilibrium path defined by equation (1) are called continuation or path following methods. They are incremental, step-wise algorithms. A typical continuation step includes the predictor and the corrector phases.

To traverse a solution path a proper parametrization is needed. Simple load control is the oldest type of parametrization. It is usually the most efficient one in regular parts of a path, and the adaptation of an iterative linear equation solver in it is straightforward. However, near the so called limit points, where the structure loses its load carrying capacity (at least locally), it can break down. At the limit point the tangent stiffness matrix is singular and the load parameter is decreasing after such a point. A remedy is to change the control from the load parameter to some of the displacement components. Selecting the controlling displacement (or component from the scaled vector containing both displacements and the load parameter) to be the largest one from the last converged increment, results in a simple and reliable continuation procedure.[16] Non-dimensionalizing of the variables is an essential point of this method. Nevertheless, it is recommendable for all other procedures, too.

A usual setting of a continuation process is to augment the discrete equilibrium equations with a single constraint equation c in the following form:

$$\left\{ \begin{array}{rcl} \boldsymbol{f}(\boldsymbol{q},\lambda) &=& \boldsymbol{0} \\ c(\boldsymbol{q},\lambda) &=& 0 \end{array} \right. . \tag{2}$$

This kind of procedures are also commonly called arc-length methods. A large class of constraint equations can be written in the form

$$c(\boldsymbol{q},\lambda) = \boldsymbol{t}^T \boldsymbol{C}\boldsymbol{n} - c_0 = 0$$

where $\boldsymbol{t}$ and $\boldsymbol{n}$ are $N+1$ dimensional vectors and c_0 is a scalar.[5,17] The weighting matrix $\boldsymbol{C}$ can be partitioned as $\mathrm{diag}(\boldsymbol{W},\alpha^2)$, where $\boldsymbol{W}$ is a positive definite or semidefinite diagonal matrix corresponding to displacements and α is a scaling factor. The weighting matrices $\boldsymbol{C}$ and $\boldsymbol{W}$ define seminorms $\|\cdot\|_C$ and $\|\cdot\|_W$ in R^{N+1} and R^N, respectively.

Using the Newton-Raphson linearization of the extended equation system (2) results in

$$\left\{ \begin{array}{rcl} \dfrac{\partial \boldsymbol{f}}{\partial \boldsymbol{q}}\delta\boldsymbol{q} + \dfrac{\partial \boldsymbol{f}}{\partial \lambda}\delta\lambda + \boldsymbol{f}(\boldsymbol{q},\lambda) &=& -\boldsymbol{K}\delta\boldsymbol{q} + \boldsymbol{p}_r\delta\lambda + \boldsymbol{f} \;=\; \boldsymbol{0} \\ \dfrac{\partial c}{\partial \boldsymbol{q}}\delta\boldsymbol{q} + \dfrac{\partial c}{\partial \lambda}\delta\lambda + c(\boldsymbol{q},\lambda) &=& \boldsymbol{c}^T\delta\boldsymbol{q} + e\delta\lambda + c \;=\; 0 \end{array} \right. . \tag{3}$$

Usually in structural analyses the tangent stiffness matrix $\boldsymbol{K}$ is symmetric. Therefore, in order to utilize the specific sparsity pattern and symmetry of the tangent stiffness matrix, the solution of the augmented equations (3) is usually performed by using the following three phase block elimination method, also known as bordering algorithm:[16,18,19]

1. solve $\boldsymbol{K}\delta\boldsymbol{q}_f = \boldsymbol{f}$ and $\boldsymbol{K}\boldsymbol{q}_p = \boldsymbol{p}_r$,

2. compute $\delta\lambda = -(c + \boldsymbol{c}^T \delta \boldsymbol{q}_f)/(e + \boldsymbol{c}^T \boldsymbol{q}_p)$,

3. update $\delta \boldsymbol{q} = \delta \boldsymbol{q}_f + \delta\lambda \boldsymbol{q}_p$.

In this format the solution of the linear equation system at phase 1 is performed by means of direct solvers.

It is now assumed that the critical point $(\boldsymbol{q}_{cr}, \lambda_{cr})$ is reached and located for prescribed accuracy between steps $k-1$ and k. Notification of new critical modes during the continuation can be obtained by monitoring the inertia of the tangent stiffness matrix. If the number of unstable modes associated with the appearance of the noticed critical point(s) is M, then

$$|\mathrm{p}(\boldsymbol{K}_k) - \mathrm{p}(\boldsymbol{K}_{k-1})| = M,$$

where $\mathrm{p}(\boldsymbol{K})$ stands for the number of positive eigenvalues. This does not necessarily mean that the lowest critical point itself is a M-fold critical point, i.e.

$$\dim(\ker \boldsymbol{K}_{cr}) = K \leq M.$$

The number of positive eigenvalues can be determined using the Sylvester law of inertia by counting the number of positive diagonal elements in the $\boldsymbol{LDL}^T$-factorized stiffness matrix. If the linear system is solved by iterative methods, the inertia of the stiffness matrix is not easily obtainable.

Multiplicity of the critical point is here defined to be the dimension of the nullspace of the tangent stiffness matrix at the critical point. Other definitions exist.[20]

An essential feature for the construction of a reliable bifurcation procedure is the determination of the number of possible solutions branches emanating from the critical point. This problem has been explored in the late 60's by Sewell,[21,22] Johns and Chilver.[23,24] Depending on the symmetry properties of the system, the maximum number of different post-buckling branches is

$$2^M - 1 \quad \text{or} \quad \tfrac{1}{2}(3^M - 1) \tag{4}$$

for a system without symmetry or perfectly symmetric, respectively. The minimum number of post-buckling paths is 1 for the former case and M for the latter. The complexity of a multi-mode buckling problem grows enormously with the multiplicity of the critical point. However, no rules for the evaluation of the number of real post-bifurcation branches exist.

3 BRANCH SWITCHING ALGORITHMS

3.1 Local perturbation approach

Allgower and Chien[12] used the local perturbation method introduced by Georg[25] to multiple bifurcation problems. The theoretical foundation of this method is based on a version

of the generalized Sard's theorem. For successful branching the choice of the perturbation vectors plays a key role. However, no specific theory or rules for the selection of the perturbation vectors was given by Allgower and Chien.[12] In their numerical examples the components in the perturbation vectors were chosen in such a way that they oscillated corresponding to those of the bifurcating solutions. This means that one should have *a priori* knowlegde of the solution of the problem which has to be solved.

A major improvement to the local perturbation algorithm is given by Huitfeldt.[13] He introduced an auxiliary equation which defines with the perturbed equilibrium equations a closed one dimensional curve in a $N+2$-dimensional space. This curve passes exactly one point on each branch (or half branch) of the unperturbed equation (1). When passing such a point the perturbation parameter τ changes sign. The problem is then to locate the zero points of the perturbation parameter τ while traversing the branch connecting curve (BCC). Thus the branch switching problem is reduced to a path following task of the augmented system

$$\boldsymbol{h}(\boldsymbol{q},\lambda,\tau) = \left\{ \begin{array}{rcl} \boldsymbol{f}(\boldsymbol{q},\lambda) + \tau \boldsymbol{b} & = & \boldsymbol{0} \\ c_b(\boldsymbol{q},\lambda,\tau) & = & 0 \end{array} \right. , \tag{5}$$

which can be solved with standard continuation algorithms. A constraint that defines a closed surface around the critical point is of spherical (elliptical) form:

$$c_b(\boldsymbol{q},\lambda,\tau) = \tfrac{1}{2}\left(\|\boldsymbol{q}-\boldsymbol{q}_{cr}\|_W^2 + \alpha^2(\lambda-\lambda_{cr})^2 + \beta^2\tau^2 - \rho^2 \right), \tag{6}$$

where α, β are scaling factors and ρ is the radius of the sphere. In principle this method does not require evaluation of the basis of the nullspace of the tangent stiffness matrix. Huitfeldt[13] used a random vector as perturbation $\boldsymbol{b}$.

There are some shortcomings with this conceptually simple and elegant method. It is not known if the branch connecting equation always defines a closed curve. It is believed, as also argued by Huitfeldt, that using a constraint which defines a closed surface, guarantees a closed path defined by the branch connecting equation (5). No mathematical proof of this is known to the authors. Secondly, there is no guarantee that all bifurcating branches have been found. This obviously depends on the choice of the perturbation. In addition, the computational expense can be very high for large problems, fortunately it grows only linearly with respect to the number of emanating branches from the bifurcation point. However, the number of branches in multimode buckling with higher multiplicity can be very large.

3.2 Asymptotic approach

In the Liapunov-Schmidt-Koiter reduction procedure the large non-linear system of equations (dimension N) is reduced into a locally equivalent system of non-linear equations dimension of which is much smaller than the original one. Basically, Koiter's initial post-buckling theory is a reduction from the infinite dimensional continuous problem into a

small system of polynomial equations. Usually, as also in Koiter's thesis,[26] the number of "post-buckling equilibrium equations" derived from the reduced potential energy expression equals the multiplicity of the buckling load. However, Koiter suggested also a method to handle nearly coincident critical loads, while Byskov and Hutchinson presented a formulation for well separated critical loads.[27] It has also been shown experimentally that the interaction between well separated critical loads can occur.[28]

In the following the generalized Liapunov-Schmidt-Koiter (LSK) technique is briefly presented.[29–31] A key point in the LSK-reduction technique is the decomposition of the ambient space into summands related to the tangent operator at the critical point:[29] [a]

$$R^N = \mathcal{N} \oplus \mathcal{N}^- , \quad \text{or} \quad R^N = \mathcal{M} \oplus \mathcal{M}^- . \tag{7}$$

In the classical formulation $\mathcal{N} = \ker \boldsymbol{K}, \mathcal{N}^- = \text{range} \boldsymbol{K}^T, \mathcal{M} = \ker \boldsymbol{K}^T, \mathcal{M}^- = \text{range} \boldsymbol{K}$. However, since the mode interaction problems are of interest, the generalized LSK-formulation[32] is adopted. Thus, it is assumed that:

$$\ker \boldsymbol{K} \subset \mathcal{N}, \quad \dim(\ker \boldsymbol{K}) = L \leq \dim \mathcal{N} = M.$$

The original equilibrium equations (1) can thus be expanded to an equivalent pair of equations

$$\boldsymbol{P}\boldsymbol{f}(\boldsymbol{q}, \lambda) = \boldsymbol{0}, \tag{8}$$

$$(\boldsymbol{I} - \boldsymbol{P})\boldsymbol{f}(\boldsymbol{q}, \lambda) = \boldsymbol{0}, \tag{9}$$

where $\boldsymbol{P}$ is a projector from $R^N \to \mathcal{M}^-$, with $\ker \boldsymbol{P} = \mathcal{M}$. Analogously $\boldsymbol{I} - \boldsymbol{P}$ is a projector from $R^N \to \mathcal{M}$ with $\ker(\boldsymbol{I} - \boldsymbol{P}) = \mathcal{M}^-$. Expression for the projector can be written as $\boldsymbol{P} = \boldsymbol{I} - \boldsymbol{\Psi}\boldsymbol{\Psi}^T$, where $\boldsymbol{\Psi}$ is a matrix containing the basevectors of $\mathcal{M}$, i.e. $\boldsymbol{\Psi} = \left[\begin{array}{ccc} \boldsymbol{\psi}_1 & \cdots & \boldsymbol{\psi}_M \end{array} \right]$.

In view of the decomposition (7a), the displacement vector onto the post-bifurcation regime can be written in the form[b]

$$\begin{aligned} \boldsymbol{q} &= \boldsymbol{q}_{cr} + a_i \boldsymbol{\phi}_i + \boldsymbol{v}(a_i, \lambda) \\ &= \boldsymbol{q}_{cr} + a_i \boldsymbol{\phi}_i + a_i \boldsymbol{v}_i + \Delta\lambda \boldsymbol{v}_\lambda + \tfrac{1}{2}\left(a_i a_j \boldsymbol{v}_{ij} + 2\Delta\lambda a_i \boldsymbol{v}_{i\lambda} + (\Delta\lambda)^2 \boldsymbol{v}_{\lambda\lambda} \right) + \cdots , \end{aligned} \tag{10}$$

where $\boldsymbol{\phi}_i$'s denote the base vectors spanning the space $\mathcal{N}$, the unknown amplitudes are a_i and $\Delta\lambda = \lambda - \lambda_{cr}$. In order to have a unique solution for $\boldsymbol{v}$ it is required to be orthogonal to the vectors $\boldsymbol{\phi}_i$, i.e. $\boldsymbol{v} \in \mathcal{N}^-$. The reduced set of equilibrium equations are obtained by substituting the field $\boldsymbol{v}$ into (9):

$$\begin{aligned} \boldsymbol{g}(a_i, \lambda) &= \boldsymbol{\Psi}^T(\boldsymbol{I} - \boldsymbol{P})\boldsymbol{f}(\boldsymbol{q}_{cr} + a_i \boldsymbol{\phi}_i + \boldsymbol{v}(a_i, \lambda), \lambda) \\ &= \boldsymbol{\Psi}^T \boldsymbol{f}(\boldsymbol{q}_{cr} + a_i \boldsymbol{\phi}_i + \boldsymbol{v}(a_i, \lambda), \lambda). \end{aligned} \tag{11}$$

[a] The residual $\boldsymbol{f}$ is a non-linear mapping from $R^N \times R$ to R^N.

[b] Einstein's summation convention is adopted for repeated lower case indexes.

Solutions for the components of $\boldsymbol{v}$ are obtained by substituting (10) into Taylor's series expansion of (8) about the critical point, i.e. $a_i = 0, \lambda = \lambda_{cr}$. As a result $\boldsymbol{v}_i$ and $\boldsymbol{v}_\lambda, \boldsymbol{v}_{\lambda\lambda}$... will vanish. The remaining second order displacement fields can be solved from equations:

$$-\boldsymbol{P}\boldsymbol{f}'\boldsymbol{v}_{ij} = \boldsymbol{P}\boldsymbol{f}''\boldsymbol{\phi}_i\boldsymbol{\phi}_j, \tag{12}$$

$$-\boldsymbol{P}\boldsymbol{f}'\boldsymbol{v}_{i\lambda} = \boldsymbol{P}\boldsymbol{f}'_{,\lambda}\boldsymbol{\phi}_i, \tag{13}$$

where the notation $\boldsymbol{f}' = \partial \boldsymbol{f}/\partial \boldsymbol{q}$ has been used. Finally, the expansion of the reduced equilibrium equations at the critical state ($a_i = 0, \lambda = \lambda_{cr}$) can be written as

$$G_i\Delta\lambda + G_{ij}a_j + \tfrac{1}{2}(G_{ijk}a_ja_k + 2G_{ij\lambda}\Delta\lambda a_j) + \tfrac{1}{6}(G_{ijk\ell}a_ja_ka_\ell + 3G_{ijk\lambda}\Delta\lambda a_ja_k) + \cdots = 0, \quad i = 1, \ldots, M \tag{14}$$

where

$$\begin{aligned}
G_i &= \boldsymbol{\psi}_i^T \boldsymbol{f}_{cr,\lambda}, \\
G_{ij} &= \boldsymbol{\psi}_i^T \boldsymbol{f}'_{cr}\boldsymbol{\phi}_j, \\
G_{ijk} &= \boldsymbol{\psi}_i^T (\boldsymbol{f}'_{cr}\boldsymbol{v}_{jk} + \boldsymbol{f}''_{cr}\boldsymbol{\phi}_j\boldsymbol{\phi}_k), \\
G_{ij\lambda} &= \boldsymbol{\psi}_i^T \boldsymbol{f}'_{cr,\lambda}\boldsymbol{\phi}_j, \\
G_{ijk\ell} &= \boldsymbol{\psi}_i^T \left[\boldsymbol{f}'_{cr}\boldsymbol{v}_{jk\ell} + \boldsymbol{f}''_{cr}(\boldsymbol{\phi}_j\boldsymbol{v}_{k\ell} + \boldsymbol{\phi}_k\boldsymbol{v}_{j\ell} + \boldsymbol{\phi}_\ell\boldsymbol{v}_{jk}) + \boldsymbol{f}'''_{cr}\boldsymbol{\phi}_j\boldsymbol{\phi}_k\boldsymbol{\phi}_\ell\right], \\
G_{ijk\lambda} &= \boldsymbol{\psi}_i^T \left[\boldsymbol{f}'_{cr}\boldsymbol{v}_{jk\lambda} + \boldsymbol{f}'_{,\lambda}\boldsymbol{v}_{jk} + \boldsymbol{f}''_{cr}(\boldsymbol{\phi}_j\boldsymbol{v}_{k\lambda} + \boldsymbol{\phi}_k\boldsymbol{v}_{j\lambda}) + \boldsymbol{f}'''_{cr,\lambda}\boldsymbol{\phi}_j\boldsymbol{\phi}_k\right].
\end{aligned}$$

Some remarks are in order. If the reference load vector does not depend on the displacement field, like in the case of dead weight loading, the higher order fields $\boldsymbol{v}_{i\lambda}, \boldsymbol{v}_{ij\lambda}$ as well as coefficients $G_{ij\lambda}, G_{ijk\lambda}$ etc. will vanish. If the space $\mathcal{N}$ equals the nullspace of the tangent matrix, then all the components G_i and G_{ij} vanish too. However, if $\dim\ker \boldsymbol{K}_{cr} = L < \dim\mathcal{N} = M$, then the product $G_{ij}a_j$ is necessarily zero in the vicinity of the critical point, since the branch directions are to be found from components $a_i, i = 1, \ldots, L$.

To summarize, after the detection of the critical point the four main steps in the LSK-reduction technique are:

1. solution of the relevant eigenmodes,
2. solution of the second-order (or higher) displacement fields,
3. computation of the coefficients of the asymptotic expansion
4. solution of the reduced set of polynomial equations.

Since the dimension of the reduced problem is very small, any robust solution scheme can be applied. Since these equations are polynomial it is possible to find all the solutions with algorithms described in detail by Morgan.[33]

A relevant problem in the initial post-buckling method is to decide how many eigenmodes are relevant in the expansion. If one interacting mode is left out from the expansion, it will appear in the second order field.[34] However, the range of validity can be extremely small in those cases.

4 NUMERICAL EXAMPLES

A well known example of multiple bifurcation is the double bifurcation of a compressed flat simply supported plate, see fig. 1. A plate with aspect ratio of $\sqrt{2}$ is chosen as a test example. Similar problem has also been analysed by Huitfeldt[13] and Lidström,[35] however, no post-bifurcation paths have been presented. They have used Hemp type in-plane boundary conditions for which the longitudinal egdes are free to move in the plane of the plate.

The Marguerre-Trefftz in-plane boundary conditions, for which the longitudinal egdes are constrained to remain straigth, are used in the present study, since the post-buckling behaviour is more interesting than it is for a plate with Hemp type BC. A uniform 20×10 quadrilateral mesh discretized by bilinear stabilized MITC type elements with drilling rotations is used (1242 dof). The stabilization parameter (shear reduction) for the MITC element has been 0.4.[36–38] Full 2×2 Gaussian integration is used in evaluation of the element stiffness matrices and internal force vector. The eigenvalue problem is solved with the block Lanczos solver BLZPACK by Marques.[39]

The loaded edges are also constrained to remain straight. The analytical buckling load has the value $P_{cr} = 4.5\pi^2 DL^{-1}$, where L is the length of the loaded side. The buckling modes corresponding to this double bifurcation load have one or two half waves in the x-axis direction. The length to thickness ratio is $L/t = 100$ and the Poisson's ratio has the value $\nu = 0.3$. In the numerical computation the value obtained is $4.39\pi^2 DL^{-1}$ interpolated from the zero point of the lowest eigenvalue of the tangent stiffness matrix, which is easily computed at the beginning of each increment by applying few inverse iterations. If an eigenvalue buckling analysis is performed, the double eigenvalue will split into two separate eigenvalues with values 4.32 and $4.40\pi^2 DL^{-1}$. Load deflection curves are shown in fig. 2.

The local perturbation approach and the branch-switching scheme based on Koiter's initial post-buckling theory are used in the computations.

For symmetric double bifurcation the maximum number of different post-buckling paths is four (4). In this particular case only two real post-bifurcation paths exist. Branching onto the post-bifurcation paths is not particularly difficult, since the deformation patterns on the branches are just like the buckling modes. The load deflection paths are shown in fig. 2. C and Q refer to the center and quarter points of the plate. However, there exists an interesting phenomena for the one half-wave mode branch. The one half-wave branch is a stable path up to the load level of $P = 11.35\pi^2 DL^{-1}$, where a change of the signature of the tangent stiffness matrix is noticed; one negative eigenvalue emerges. Deformation mode changes gradually from one half-wave buckle to three half-

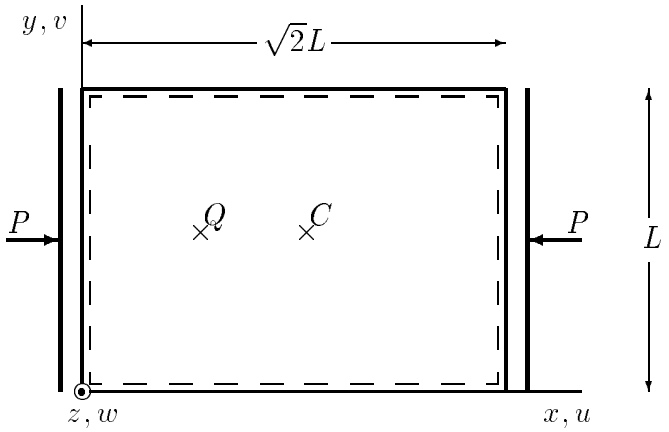

Figure 1: Simply supported plate.

wave buckle and the load bearing capacity decreases. At the load level of $P = 7.84\pi^2 DL^{-1}$ there exist two closely spaced changes in the number of negative eigenvalues, first from one to two and then back from two to one, after which the load starts to increase and the deformation mode is fully developed three half-wave buckle. After the load level of $P = 9.27\pi^2 DL^{-1}$ the three half-wave mode branch becomes stable, see fig. 2. Thus, under pure load control the plate would exhibit a mode jump from one half-wave buckle to three half-wave buckle. Deformation plots are appended in fig. 5 and the membrane stress resultant distributions in fig. 6.

The initially two half-wave branch is stable up to load level $P \approx 37\pi^2 DL^{-1}$, where one unstable mode appears.

For the Huitfeldt's method different perturbation loads are tested. As already pointed out, the perturbation load should cause deflections in the direction of the branch tangents. If not so, the BCC curve can be closed but some branches are missing. Another type of problem exist with the local perturbation approach. Even if the branch connecting constraint (6) defines a closed surface around the critical point, the BCC tracing seems to produce *a closed curve on the surface of the constraint, not passing the point of departure.* These failures are demonstrated in detail by Kouhia and Mikkola.[40]

The main computational labor in the LSK-reduction technique is the solution of the eigenvalue problem. Computing the second-order fields, coefficients of the reduced set of equations as well as solving the polynomial system are orders of magnitude less time consuming than solving the eigenproblem. For Huitfeldt's local perturbation approach the main work is to traverse the branch connecting curve, which is a standard path following routine and thus expensive for large systems. Solution times [c] of the branch switching processes of this particular example are of the order of 50 s for Huitfeldt's approach

[c]The CPU-times are on a Digital AlphaServer 8400 at the Center for Scientific Computing, Espoo, Finland.

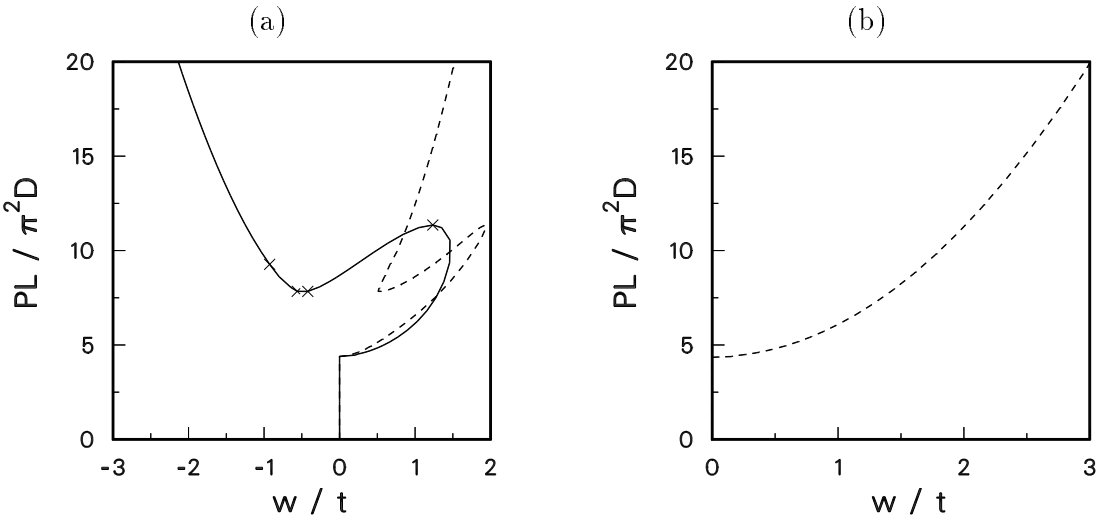

Figure 2: Out of plane deflections vs. load curves: (a) initially one half-wave branch, (b) initially two half-wave branch; solid line = w_C dashed line = w_Q. Load steps where change in signature of the tangent stiffness matrix on the post-buckling branch occurs are denoted by ×.

and only 2 s for the LSK-reduction based technique. To trace one complete equilibrium curve shown in fig. 2 took approximately 100 s and 55 s, respectively (the two half-wave path). In these computations the primary path is traced with 3 steps and 23 steps on the post-buckling path.

An example of three mode interaction is a simply supported T-beam loaded by a transverse force at midspan and in the direction that induced compression in the flange. This particular example has been extensively studied by Menken and his co-workers at the Eindhoven University of Technology.[41–43] The material of the beam is aluminium (E=70 GPa, ν=0.3) and the dimensions of the cross-section are (see fig. 3): flange: width 30 mm, thickness 0.5 mm; web: height 50 mm, thickness 2 mm. Experiments were carried out with several lengths of the beam. For the shorter beams local flange buckling would occur first, while buckling is initiated by an overall lateral-torsional mode for the longer ones. The local buckling load is strongly influenced by the free width of the flange, therefore the overlap between flange and web is modelled by orthotropic elements having high rigidity in transverse direction. However, this will produce highly ill-conditioned stiffness matrices, the spectral condition number of the tangent stiffness matrice varied within the range of $10^{15} - 10^{17}$ on the computed paths.

In earlier studies[34, 42, 43] the beam has been modelled by spline finite strips; all displacements are interpolated with B_3-splines in the longitudinal direction and in transverse direction linear interpolation is used for membrane displacements and the cubic Hermitian polynomials for the out of plane displacement and the kinematical model is based on the classical Kirchhoff-Love hypothesis. In the above mentioned references the model consists of 22 strips divided into 40 sections. In this study similar kind of a finite element

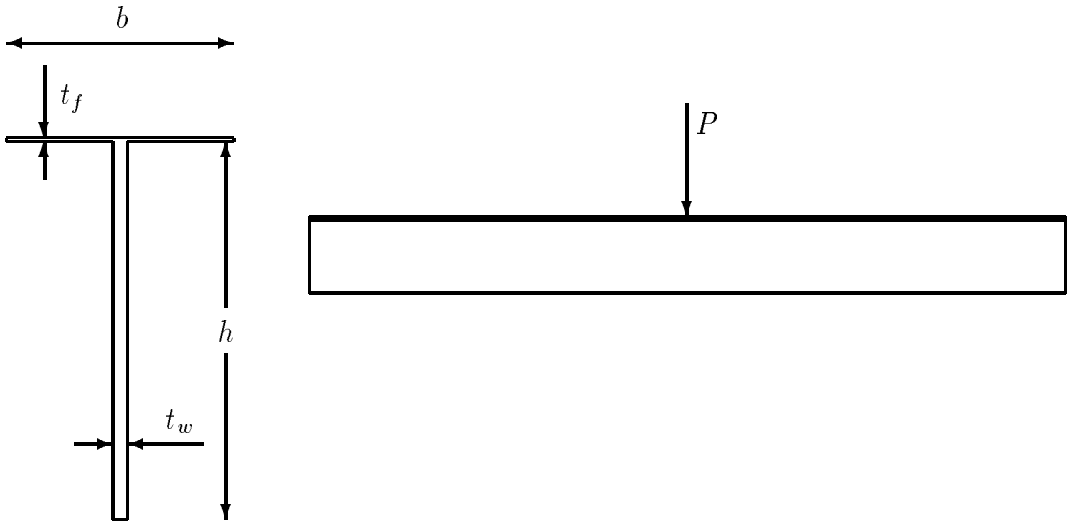

Figure 3: Simply supported T-beam.

mesh is used with 880 quadrilateral facet-type shell elements, in which the Lyons-Crisfield DKQ-element[44] is used for the bending part and the Hughes-Brezzi-Allman type membrane interpolation with drilling rotations.

Only beams having the lengths of 520 and 620 mm are considered. In the linear buckling analysis the overall buckling mode and the local flange buckles appear independently. However, in the non-linear analysis the second mode is a combination of the local and overall lateral-torsional buckling modes, while the first mode is a pure local mode, antisymmetric with respect to the web. Also the critical load for the 520 mm long beam appeared to be smaller than the linear buckling analysis prediction. The bifurcation occurs within the step from the load level of 1110 N to 1240 N (two negative eigenvalues), and the estimated value is 1146 N. Moreover, the flange deflections for both two lowest modes are antisymmetric with respect to the web. Therefore, the combination of the fisrt and second modes will not leave the other flange unbuckled and thus a higher mode is required in order to have a proper predictor onto the post-buckling branch (sixth mode[40]).

There are convergence problems near the bifurcation point as well on the primary path as on the bifurcated path. True Newton-Raphson with the orthogonal trajectory process is used and mostly 2-4 corrector iteration are needed, except near the bifurcation point where the iteration number jumps to 10-15 during the step where the bifurcation point is jumped over. This is most probably due to the clustering of the eigenvalues near the bifurcation point. Also the prediction step onto the branch requires more iterations; this can be due to the relatively large jump to the lower load level, and due to the ill-conditioning of the global system.

For the 620 mm long beam the behaviour is different. The overall lateral-torsional mode is the lowest one, but there exists a strong interaction with the local modes. In

the asymptotic analysis assuming linear pre-buckling behaviour, there is a secondary bifurcation near the primary one, and a drop in load occurs. However, in the non-linear analysis the secondary mode could not be detected, perhaps due to the eigenmode mixing and the predictor onto the branch is a prediction beyond the secondary bifurcation onto the secondary post-buckling branch. However, it could be almost impossible to detect in the full non-linear analysis due to the nearness from the primary bifurcation point. Therefore it could be usefull to use methods which directly computes the secondary bifurcations.[45]

In the non-linear analysis the estimated buckling load is 931 N which is quite close to the linear buckling analysis prediction 924 N[40] and the immediate load drop on the bifurcating branch is 143 N. The load deflection curves are shown in fig. 4.

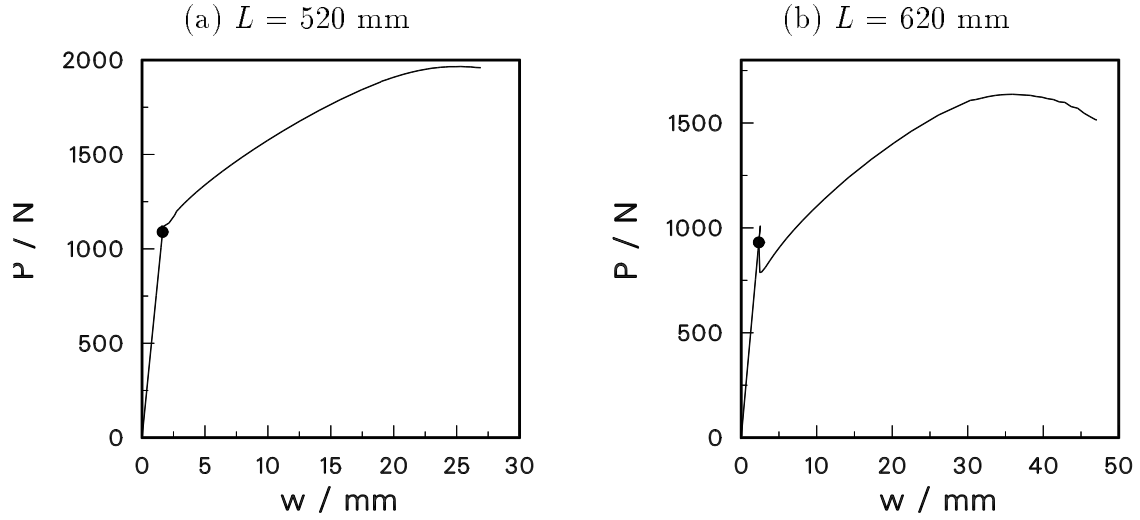

Figure 4: Vertical deflection under the point load vs. load.

.

5 CONCLUDING REMARKS

So far all existing branch switching techniques which can be used in multiple bifurcation problems have some annoying features. In principle Huitfeldt's approach for traversing the branch connecting curve requires only a path following procedure, no other specific algorithms are needed. This is in contrast to other branch switching methods which requires the basis of the nullspace of the tangent stiffness matrix, i.e. the eigenmodes. However, in practise also with Huitfeldt's approach, some knowledge on the critical eigenmodes seems to be necessary in order to construct a proper perturbation load.

To solve the eigenvalue problem at the critical point is the most time consuming part of the proposed branch switching algorithm which uses the Koiter-type reduction method. However, it is shown to be much faster than Huitfeldt's local perturbation approach.

As mentioned before, the range of applicability of the Lyapunov-Schmidt-Koiter type reduction can be very narrow due in the case that some relevant interacting modes are left out from the series expansion. However, this usually manifests itself by the appearance of secondary bifurcations close to the primary one. It is extremely difficult to automate the selection of the relevant buckling modes. Thus, at this moment human expertise in performing stability computations involving interactive buckling phenomena is crucial for successful analysis.

REFERENCES

[1] W.C. Rheinboldt. Numerical methods for a class of finite dimensional bifurcation problems. *SIAM Journal on Numerical Analysis*, **15**, 1–11 (1978).

[2] E. Riks. An incremental approach to the solution of snapping and buckling problems. *International Journal of Solids and Structures*, **15**, 529–551 (1979).

[3] W. Wagner and P. Wriggers. A simple method for the calculation of postcritical branches. *Engineering Computation*, **5**, 103–109 (1988).

[4] D.J. Allman. Calculation of the stable equilibrium paths of discrete conservative systems with singular points. *Computers and Structures*, **32**, 1045–1054 (1989).

[5] R. Kouhia and M. Mikkola. Tracing the equilibrium path beyond simple critical points. *International Journal for Numerical Methods in Engineering*, **28**, 2933–2941 (1989).

[6] B.-Z. Huang and S.N. Atluri. A simple method to follow post-buckling paths in finite element analysis. *Computers and Structures*, **57**(3), 477–489 (1995).

[7] E.L. Allgower and H. Schwetlick. A general view of minimally extended systems for simple bifurcation points. *ZAMM*, **77**(2), 83–97 (1997).

[8] R. Seydel. Numerical computation of branch points in nonlinear equations. *Numer. Math.*, **33**, 339–352 (1979).

[9] P. Wriggers and J.C. Simo. A general procedure for the direct computation of turning and bifurcation problems. *Computer Methods in Applied Mechanics and Engineering*, **30**, 155–176 (1990).

[10] H.B. Keller. Numerical solution of bifurcation and nonlinear eigenvalue problems. In P.H. Rabinowitz, editor, *Applications of Bifurcation Theory*, pages 359–384. Academic Press, (1977).

[11] R.B. Kearfott. Some general bifurcation techniques. *SIAM Journal on Scientific and Statistical Computing*, **4**, 52–68 (1983).

[12] E.L. Allgower and C.-S. Chien. Continuation and local perturbation for multiple bifurcations. *SIAM Journal on Scientific and Statistical Computing*, **7**, 1265–1281 (1986).

[13] J. Huitfeldt. Nonlinear eigenvalue problems - prediction of bifurcation points and branch switching. Technical Report 17, Department of Computer Sciences, Chalmers University of technology, (1991).

[14] J.C. Wohlever and T.J. Healey. A group theoretic approach to the global bifurcation

analysis of an axially compressed cylindrical shell. *Computer Methods in Applied Mechanics and Engineering*, **122**, 315–349 (1995).

[15] J.C. Wohlever. A group theoretic approach to the global bifurcation analysis of symmetric structures using a standard finite element package. submitted in *Computer Methods in Applied Mechanics and Engineering*, (1997).

[16] W.C. Rheinboldt. *Numerical Analysis of Parametrized Nonlinear Equations*. Wiley, (1986).

[17] R. Kouhia and M. Mikkola. Strategies for structural stability analyses. In N.E. Wiberg, editor, *Advances in Finite Element Technology*, pages 254–278, (1995).

[18] H.B. Keller. The bordering algorithm and path following near singular points of higher nullity. *SIAM Journal on Scientific and Statistical Computing*, **4**, 573–582 (1983).

[19] K.H. Schweizerhof and P. Wriggers. Consistent linearization for path following methods in nonlinear FE analysis. *Computer Methods in Applied Mechanics and Engineering*, **59**, 261–279 (1986).

[20] L. Bauer, H.B. Keller, and E.L. Reiss. Multiple eigenvalue lead to secondary bifurcation. *SIAM Review*, **17**(1), 101–122 (1975).

[21] M.J. Sewell. A general theory of equilibrium paths through critical points. *Proceedings of the Royal Society - A*, **306**, 201–238 (1968).

[22] M.J. Sewell. On the branching of equilibrium paths. *Proceedings of the Royal Society - A*, **315**, 499–518 (1970).

[23] K.C. Johns and A.H. Chilver. Multiple path generation at coincident branching points. *International Journal of Engineering Science*, **13**, 899–910 (1971).

[24] K.C. Johns. Simultaneous buckling in symmetric structural systems. *Engineering Mechanics Division, Proceedings of the American Society of Civil Engineers*, **98**, 835–848 (1972).

[25] K. Georg. On tracing an implicitely defined curve by quasi-newton steps and calculating bifurcation by local perturbations. *SIAM Journal on Scientific and Statistical Computing*, **2**, 35–50 (1981).

[26] W.T. Koiter. *Over de stabiliteit van het elastisch evenwicht* (in Dutch). PhD thesis, Technische Hogeschool, Delft, (1945). English tranlations: NASA TT F10, 833 (1967) and AFFDL, TR-7025 (1970).

[27] E. Byskov and J.W. Hutchinson. Mode interaction in axially stiffened cylindrical shells. *AIAA Journal*, **15**, 941–948 (1977).

[28] C.M. Menken, W.J. Groot, and G.A.J. Stallenberg. Interactive buckling of beams in bending. *Thin-Walled Structures*, **12**, 415–434 (1991).

[29] M. Golubitsky and D.G. Schaeffer. *Singularities and Groups in Bifurcation Theory*, volume 1. Springer-Verlag, (1985).

[30] N. Triantafyllidis and R. Peek. On stability and the worst imperfection shape in solids with nearly simultaneous eigenmodes. *International Journal of Solids and Structures*, **29**(18), 2281–2299 (1992).

[31] R. Peek and M. Kheyrkhahan. Postbuckling behaviour and imperfection sensitivity of elastic structures by the Lyapunov-Schmidt-Koiter approach. *Computer Methods in Applied Mechanics and Engineering*, **108**, 261–279 (1993).

[32] A.D. Jepson and A. Spence. On a reduction process for nonlinear equations. *SIAM Journal on Matrix Analysis*, **20**(1), 39–56 (1989).

[33] A. Morgan. *Solving Polynomial Systems Using Continuation for Engineering and Scientific Problems*. Prentice-Hall, (1987).

[34] R. Kouhia, C.M. Menken, M. Mikkola, and G.-J. Schreppers. Computing and understanding interactive buckling. In R.A.E. Mäkinen and P. Neittaanmäki, editors, *Proceedings of the 5th Finnish Mechanics Days*, pages 53–61, (1994).

[35] T. Lidström. *Computational methods for finite element instability analyses*. PhD thesis, Royal Institute of Technology, Department of Structural Engineering, (1996).

[36] M. Lyly, R. Stenberg, and T. Vihinen. A stable bilinear element for the Reissner-Mindlin plate model. *Computer Methods in Applied Mechanics and Engineering*, **110**, 343–357 (1993).

[37] D.J. Allman. A compatible triangular element including vertex rotations for plane elasticity analysis. *Computers and Structures*, **19**, 1–8 (1984).

[38] T.J.R. Hughes and F. Brezzi. On drilling degrees of freedom. *Computer Methods in Applied Mechanics and Engineering*, **72**, 105–121 (1989).

[39] O.A. Marques. BLZPACK: description and users guide. Technical Report TR/PA/95/30, CERFACS, (1995).

[40] R. Kouhia and M. Mikkola. Tracing the equilibrium path beyond compound critical points. manuscript, submitted for publication, (1998).

[41] W.J. Groot C.M. Menken and R. Petterson. Experiments on coupled instabilities. In *10th Int. Conf. on Experimental Mech.*, (1994).

[42] C.M. Menken, R. Kouhia, and W.J. Groot. An investigation into non-linear interaction between buckling modes. *Thin-Walled Structures*, **19**, 129–145 (1994).

[43] C.M. Menken, G. Schreppers, W.J. Groot, and R. Petterson. Computing and experimenting in buckling. In M. Papadrakakis and H.B. Topping, editors, *Advances in Computational Mechanics*, pages 69–75. CIVIL-COMP Ltd., (1994).

[44] M.A. Crisfield. *Finite Elements and Solution Procedures for Structural Analysis, Volume 1: Linear Analysis*. Pineridge Press, Swansea, U.K., (1986).

[45] B. Wu. Numerical non-linear analysis of secondary buckling in stability problems. *Computer Methods in Applied Mechanics and Engineering*, **120**, 183–193 (1995).

$$P = 4.75\pi^2 DL^{-1}$$

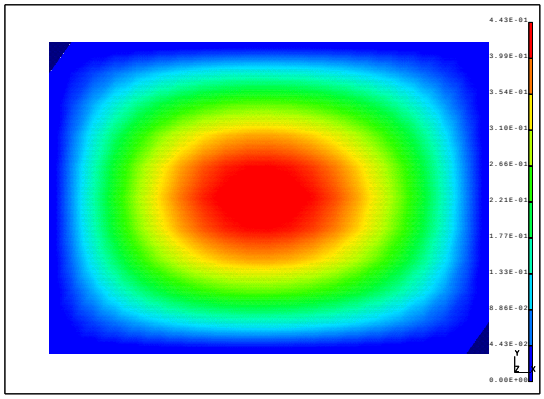

$$P = 8.5\pi^2 DL^{-1}$$

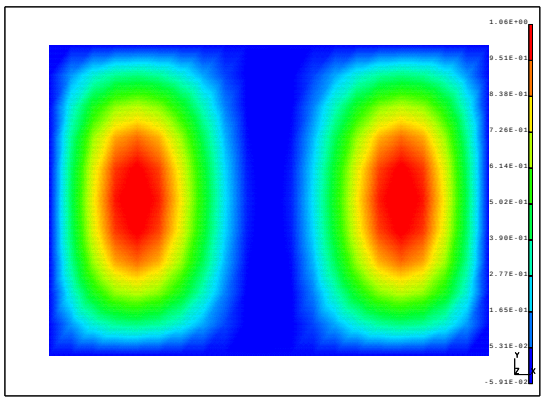

$$P = 20.0\pi^2 DL^{-1}$$

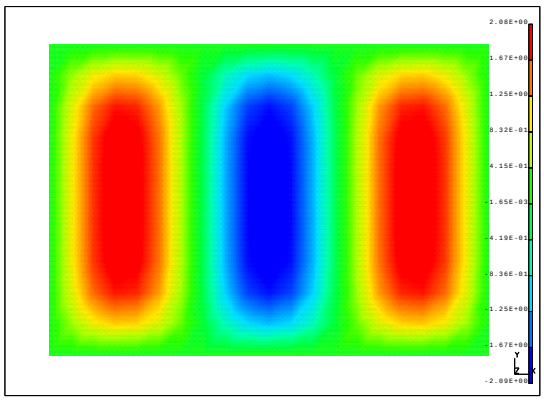

Figure 5: Out of plane displacement plots of compressed simply supported plate at three load levels on the initially one half-wave buckle post-buckling path; Marguerre-Trefftz type boundary conditions.

N_x

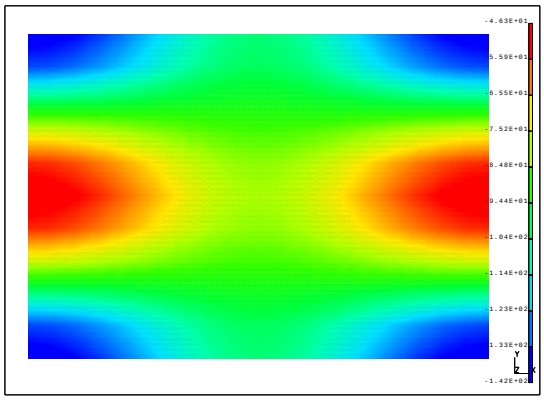

N_y

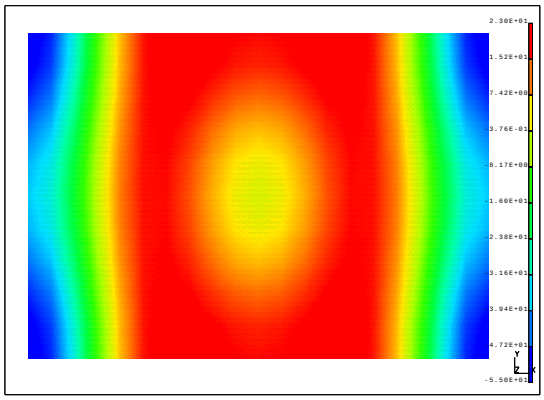

N_{xy}

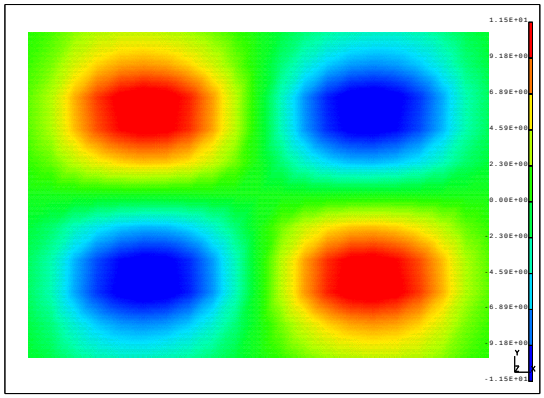

Figure 6: Membrane stress resultants at load level $P = 8.5\pi^2 DL^{-1}$ on the one half-wave branch.